Diagrammatic Monte Carlo simulation of quantum impurity models – weak and strong coupling approach

Philipp Werner

Columbia University, 538 West, 120th Street, New York, NY 10027, USA

(Dated: May 2008)

I. INTRODUCTION

An impurity model describes an atom or molecule embedded in some host or *bath*, with which it can exchange electrons. This exchange of electrons allows the impurity to make transitions between different quantum states, and leads to a non-trivial dynamics. Therefore, despite the zero dimensional nature (which makes impurity problems computationally much more tractable than fermionic lattice models), their numerical simulation remains a challenging task. Methods such as exact diagonalization or numerical RG, which explicitly treat a finite number of bath states, work well for single orbital models. However, because the number of bath states must be increased proportional to the number or orbitals, the computational effort grows exponentially with system size, and requires severe truncations of the bath already for two orbitals. Monte Carlo methods have the advantage that the bath is integrated out and thus the (infinite) size of the bath Hilbert space does not affect the simulation. While restricted to finite temperature, Monte Carlo methods are thus the method of choice for the solution of large multi-orbital or cluster impurity problems. Furthermore, over the last few years, significant progress has been achieved (both in terms of efficiency and flexibility) with the development of diagrammatic Monte Carlo techniques. These notes provide an overview over two recently developed methods – a weak-coupling approach, which scales favorably with system size and allows the efficient simulation of large impurity clusters, and a strong-coupling approach, which can handle impurity models with strong interactions.

For simplicity, we will focus on the single orbital Anderson impurity model defined by the Hamiltonian $H = H_0 + H_U + H_{\text{bath}} + H_{\text{mix}}$ with

$$H_0 = -(\mu - U/2)(n_\uparrow + n_\downarrow), \tag{1}$$

$$H_U = U(n_\uparrow n_\downarrow - (n_\uparrow + n_\downarrow)/2), \tag{2}$$

$$H_{\text{bath}} = \sum_{\sigma,p} \epsilon_p a^\dagger_{p,\sigma} a_{p,\sigma}, \tag{3}$$

$$H_{\text{mix}} = \sum_{\sigma,p} (V_p^\sigma d^\dagger_\sigma a_{p,\sigma} + h.c.). \tag{4}$$

Here, $H_0 + H_U \equiv H_{\text{loc}}$ describes the impurity with creation operators $d^\dagger_\sigma$, H_{bath} a non-interacting bath of electrons (labeled by quantum numbers p) with creation operators $a^\dagger_{p,\sigma}$, and H_{mix} controls the exchange of electrons between the impurity and the bath. The transition amplitudes V_p^σ are called *hybridizations*.

The partition function Z is given by

$$Z = Tr\left[e^{-\beta H}\right], \tag{5}$$

with β the inverse temperature, and $Tr = Tr_d Tr_a$ the trace over all the impurity and bath states. By "solving the impurity model" we essentially mean computing the impurity Green's function $(0 < \tau < \beta)$

$$g(\tau) = \frac{1}{Z} Tr\left[e^{-(\beta-\tau)H} d e^{-\tau H} d^\dagger\right]. \tag{6}$$

which we choose to be positive.

Diagrammatic Monte Carlo simulation relies on an expansion of the partition function into a series of diagrams and the stochastic sampling of (collections) of these diagrams. We represent the partition function as a sum (or, more precisely, integral) of configurations c with weight w_c,

$$Z = \sum_c w_c, \tag{7}$$

and implement a random walk $c_1 \to c_2 \to c_3 \to \ldots$ in configuration space in such a way that each configuration can be reached from any other in a finite number of steps (*ergodicity*) and that *detailed balance* is satisfied,

$$|w_1| p(c_1 \to c_2) = |w_2| p(c_2 \to c_1). \tag{8}$$

This assures that each configuration is visited with a probability proportional to $|w_c|$ and one can thus obtain an estimate for the Green's function from a finite number N of measurements:

$$g \approx \frac{\sum_{i=1}^{N} |w_{c_i}| \text{sign}_{c_i} g_{c_i}}{\sum_{i=1}^{N} |w_{c_i}| \text{sign}_{c_i}} = \frac{\langle \text{sign} \cdot g \rangle}{\langle \text{sign} \rangle}. \tag{9}$$

The error on this estimate decreases like $1/\sqrt{N}$. If the average sign of the configurations is small and decreases exponentially with decreasing temperature, the algorithm suffers from a sign problem.

The first step in the diagrammatic expansion is to rewrite the partition function as a time ordered exponential using some interaction representation. We split the Hamiltonian into two parts, $H = H_1 + H_2$ and define the time dependent operators in the interaction picture as $O(\tau) = e^{\tau H_1} O e^{-\tau H_1}$. We furthermore introduce the operator $A(\beta) = e^{\beta H_1} e^{-\beta H}$ and write the partition function as $Z = Tr[e^{-\beta H_1} A(\beta)]$. The operator $A(\beta)$ satisfies $dA/d\beta = e^{\beta H_1}(H_1 - H)e^{-\beta H} = -H_2(\beta)A(\beta)$ and can be expressed as $A(\beta) = T \exp[-\int_0^\beta d\tau H_2(\tau)]$.

In a second step, the time ordered exponential is expanded into a power series,

$$\begin{aligned} Z &= Tr\left[e^{-\beta H_1} T e^{-\int_0^\beta d\tau H_2(\tau)}\right] \\ &= \sum_{n=0}^{\infty} \int_0^\beta d\tau_1 \ldots \int_{\tau_{n-1}}^\beta d\tau_n Tr\left[e^{-(\beta-\tau_n)H_1}(-H_2)\ldots e^{-(\tau_2-\tau_1)H_1}(-H_2)e^{-\tau_1 H_1}\right], \end{aligned} \tag{10}$$

which is a representation of the partition function of the form (7), namely the sum of all configurations $c = \{\tau_1, \ldots, \tau_n\}$, $n = 0, 1, \ldots$, $\tau_i \in [0, \beta)$ with weight

$$w_c = Tr\left[e^{-(\beta-\tau_n)H_1}(-H_2)\ldots e^{-(\tau_2-\tau_1)H_1}(-H_2)e^{-\tau_1 H_1}\right]d\tau^n. \tag{11}$$

In the following I will discuss in detail two complementary diagrammatic Monte Carlo algorithms, namely

1. a *weak-coupling* approach, based on an expansion of Z in powers of the interaction U, and on an interaction representation in which the time evolution is determined by the *quadratic* part $H_0 + H_{\text{bath}} + H_{\text{mix}}$ of the Hamiltonian,

2. a *"strong-coupling"* approach, based on an expansion of Z in powers of the impurity-bath hybridization V, and an interaction representation in which the time evolution is determined by the *local* part $H_0 + H_U + H_{\text{bath}}$ of the Hamiltonian.
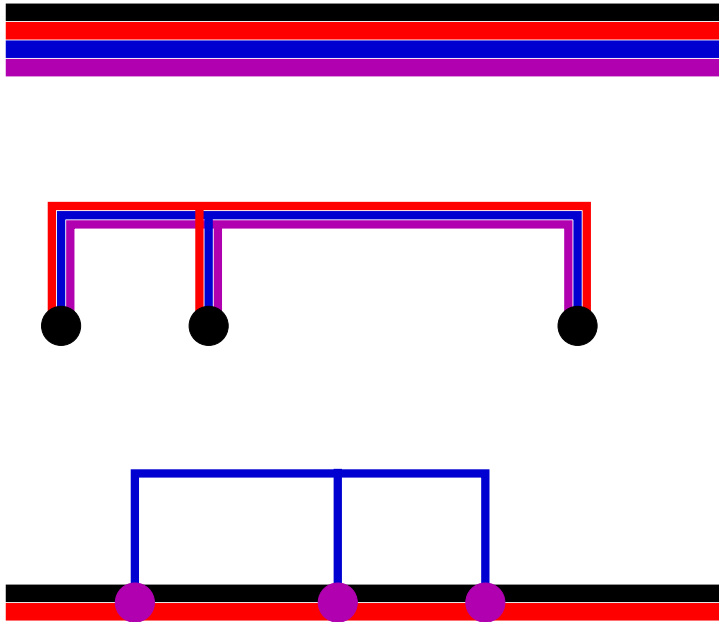
FIG. 1: An artists rendering of the weak- and strong-coupling diagrammatic algorithms. Top: partition function. The black, red, blue and cyan colors correspond to H_U, H_0, H_{bath} and H_{mix}, respectively. Middle: weak-coupling diagram. Bottom: "strong-coupling" diagram. Thick horizontal lines represent a trace, thin lines connecting dots a determinant.

II. WEAK-COUPLING APPROACH

The first diagrammatic impurity solver, proposed by Rubtsov *et al.* three years ago [1], is based on an expansion in $H_2 = H_U$. Here, I will discuss a variant of the weak coupling approach, worked out very recently by Gull *et al.* [2], which combines the weak-coupling expansion with an auxiliary field decomposition. This "continuous-time auxiliary field mehtod" is an adaptation of an algorithm by Rombouts *et al.* [3] for lattice models (which to my knowledge is the first diagrammatic Monte Carlo algorithm for fermions) and in some respects similar to the well-known Hirsch-Fye algorithm [4].

A. Monte Carlo configurations

Following Rombouts and collaborators, we define $H_2 = H_U - K/\beta$ and $H_1 = H - H_2 = H_0 + H_{\text{bath}} + H_{\text{mix}} + K/\beta$, with K some arbitrary (positive) constant. Equation (10) then gives the expression for the partition function after expansion in H_2, and (11) the weight of

a configuration of n *"interaction vertices"*. At this stage, we expand our configuration space by decoupling each interaction vertex using the decoupling formula proposed in Ref. [3],

$$-H_2 = K/\beta - U(n_\uparrow n_\downarrow - (n_\uparrow + n_\downarrow)/2) = \frac{K}{2\beta} \sum_{s=-1,1} e^{\gamma s(n_\uparrow - n_\downarrow)}, \tag{12}$$

$$\cosh(\gamma) = 1 + (\beta U)/(2K). \tag{13}$$

This formula can easily be verified by checking the four states $|0\rangle$, $|\uparrow\rangle$, $|\downarrow\rangle$, and $|\uparrow\downarrow\rangle$. The configuration space is now the collection of all possible spin configurations on the imaginary time interval $[0, \beta)$: $c = \{\{\tau_1, s_1\}, \dots, \{\tau_n, s_n\}\}$, $n = 0, 1, \dots$, $\tau_i \in [0, \beta)$, $s_i = \pm 1$. These configurations have weight

$$w_c = Tr\left[e^{-(\beta-\tau_n)H_1}e^{\gamma s_n(n_\uparrow - n_\downarrow)} \dots e^{-(\tau_2-\tau_1)H_1}e^{\gamma s_1(n_\uparrow - n_\downarrow)}e^{-\tau_1 H_1}\right]\left(\frac{Kd\tau}{2\beta}\right)^n. \tag{14}$$

All the operators in the trace are quadratic in c and a, so we can first separate the spin components and then proceed to the analytical calculation of the trace. Introducing $H_1^\sigma = -\mu(n_\sigma - U/2) + \sum_p \epsilon_p a_{p,\sigma}^\dagger a_{p,\sigma} + \sum_p(V_{\sigma,p} c_\sigma^\dagger a_{p,\sigma} + h.c.)$, which is the Hamiltonian of the non-interacting impurity model, the trace in Eq. (14) becomes ($Z_{0,\sigma} = Tr[e^{-\beta H_1^\sigma}]$)

$$Tr\left[\dots\right] = e^{-K}\prod_\sigma Tr\left[e^{-(\beta-\tau_n)H_1^\sigma}e^{\gamma s_n \sigma n_\sigma} \dots e^{-(\tau_2-\tau_1)H_1^\sigma}e^{\gamma s_1 \sigma n_\sigma}e^{-\tau_1 H_1^\sigma}\right]. \tag{15}$$

Using the identity $e^{\gamma s \sigma n_\sigma} = e^{\gamma s \sigma}c_\sigma^\dagger c_\sigma + c_\sigma c_\sigma^\dagger = e^{\gamma s \sigma} - (e^{\gamma s \sigma} - 1)c_\sigma c_\sigma^\dagger$, the trace factors can be expressed in terms of non-interacting impurity Green's functions and evaluated using Wick's theorem. For example, at first order, we find

$$Tr\left[e^{-(\beta-\tau_1)H_1^\sigma}(e^{\gamma s \sigma} - (e^{\gamma s \sigma} - 1)c_\sigma c_\sigma^\dagger)e^{-\tau_1 H_1}\right] = Z_{0,\sigma}(e^{\gamma s \sigma} - g_{0\sigma}(0_+)(e^{\gamma s \sigma} - 1)). \tag{16}$$

For n spins, this expression generalizes to

$$Tr\left[e^{-(\beta-\tau_n)H_1^\sigma}e^{\gamma s_n \sigma n_\sigma} \dots e^{-(\tau_2-\tau_1)H_1^\sigma}e^{\gamma s_1 \sigma n_\sigma}e^{-\tau_1 H_1}\right] = Z_{0,\sigma} \det N_\sigma^{-1}(\{s_i, \tau_i\}), \tag{17}$$

where N_σ is a $(n \times n)$ matrix defined by the location of the decoupled interaction vertices, the spin orientations and non-interaction Green's function:

$$N_\sigma^{-1}(\{s_i, \tau_i\}) \equiv e^{\Gamma_\sigma} - G_{0\sigma}\left(e^{\Gamma_\sigma} - I\right). \tag{18}$$

The notation is $e^{\Gamma_\sigma} \equiv \text{diag}(e^{\gamma \sigma s_1}, \dots, e^{\gamma \sigma s_n})$, $(G_{0\sigma})_{i,j} = g_{0\sigma}(\tau_i - \tau_j)$ for $i \neq j$, $(G_{0\sigma})_{i,i} = g_{0\sigma}(0_+)$. Combining Eqs. (14), (15), (17) and (18) we thus obtain the following weight for configuration $c = \{\{\tau_1, s_1\}, \dots, \{\tau_n, s_n\}\}$:

$$w_c = e^{-K}\left(\frac{Kd\tau}{2\beta}\right)^n \prod_\sigma Z_{0\sigma} \det N_\sigma^{-1}(\{s_i, \tau_i\}). \tag{19}$$
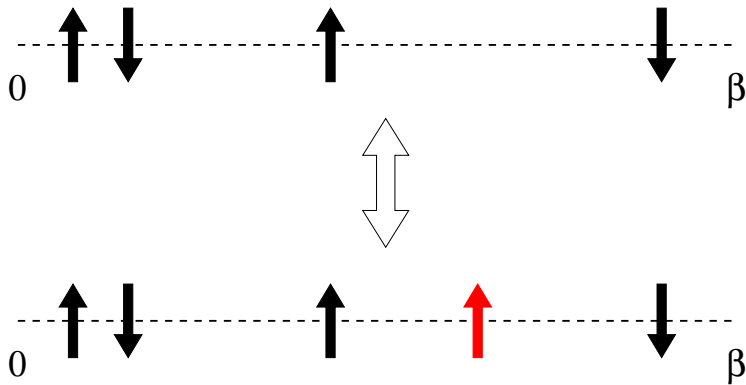
FIG. 2: Local update in the continuous-time auxiliary field method. The dashed line represents the imaginary time interval $[0, \beta)$. We increase the perturbation order by adding a spin with random orientation at a random time. The perturbation order is decreased by removing a randomly chosen spin.

B. Sampling procedure and detailed balance

For ergodicity it is sufficient to insert/remove spins with random orientation at random times, because this allows in principle to generate all possible configuration. Furthermore, the random walk in configuration space must satisfy the detailed balance condition (8). Splitting the probability to move from configuration c_i to configuration c_j into a probability to *propose* the move and a probability to *accept* it,

$$p(c_i \to c_j) = p^{\mathrm{prop}}(c_i \to c_j)p^{\mathrm{acc}}(c_i \to c_j), \tag{20}$$

we arrive at the condition

$$\frac{p^{\mathrm{acc}}(c_i \to c_j)}{p^{\mathrm{acc}}(c_j \to c_i)} = \frac{p^{\mathrm{prop}}(c_j \to c_i)}{p^{\mathrm{prop}}(c_i \to c_j)} \frac{|w(c_j)|}{|w(c_i)|}. \tag{21}$$

There is some flexibility in choosing the proposal probabilities. A reasonable choice for the insertion/removal of a spin is the following (illustrated in Fig. 2):

- *Insertion*

  Pick a random time in $[0, \beta)$ and a random direction for the new spin:
  $p^{\mathrm{prop}}(n \to n+1) = (1/2)(d\tau/\beta)$

- *Removal*

  Pick a random spin: $p^{\mathrm{prop}}(n+1 \to n) = 1/(n+1)$.

For this choice, the ratio of acceptance probabilities becomes

$$\frac{p^{\mathrm{acc}}(n \to n+1)}{p^{\mathrm{acc}}(n+1 \to n)} = \frac{K}{n+1} \prod_{\sigma=\uparrow,\downarrow} \frac{|\det(N_\sigma^{(n+1)})^{-1}|}{|\det(N_\sigma^{(n)})^{-1}|}, \tag{22}$$

and the random walk can thus be implemented for example on the basis of the Metropolis algorithm, *ie* the proposed move from n to $n \pm 1$ is accepted with probability

$$\min\left[1, \frac{p^{\mathrm{acc}}(n \to n \pm 1)}{p^{\mathrm{acc}}(n \pm 1 \to n)}\right]. \tag{23}$$

C. Determinant ratios and fast matrix updates

From Eq. (22) it follows that each update requires the calculation of a ratio of two determinants. Computing the determinant of a matrix of size $(n \times n)$ is an $O(n^3)$ operation (*LU* decomposition). The important thing to realize is that each insertion or removal of a spin merely changes one row and one column of the matrix N_σ^{-1}. We will now show that it is therefore possible to evaluate the ratio in Eq. (22) in a time $O(n^2)$ (insertion) or $O(1)$ (removal).

The objects which are stored and manipulated during the simulation are, besides the lists of the times $\{\tau_i\}$ and spins $\{s_i\}$, the matrices $N_\sigma = (e^{\Gamma_\sigma} - G_{0\sigma}(e^{\Gamma_\sigma} - I))^{-1}$. Inserting a spin adds a new row and column to N_σ^{-1}. Following the notation of Refs. [2, 5], we define the blocks (omitting the σ index)

$$(N^{(n+1)})^{-1} = \begin{pmatrix} (N^{(n)})^{-1} & Q \\ R & S \end{pmatrix}, \quad N^{(n+1)} = \begin{pmatrix} \tilde{P} & \tilde{Q} \\ \tilde{R} & \tilde{S} \end{pmatrix}, \tag{24}$$

where Q, R, S denote $(n \times 1)$, $(1 \times n)$, and (1×1) matrices, respectively, which contain the contribution of the added spin. The determinant ratio needed for the acceptance/rejection probability is then given by

$$\frac{\det(N^{(n+1)})^{-1}}{\det(N^{(n)})^{-1}} = \frac{1}{\det \tilde{S}} = S - [R][N^{(n)}Q]. \tag{25}$$

As we store $N^{(n)}$, computing the acceptance/rejection probability of an insertion move is an $O(n^2)$ operation. If the move is accepted, the new matrix $N^{(n+1)}$ is computed out of

$N^{(n)}, Q, R$, and S, also in a time $O(n^2)$:

$$\tilde{S} = (S - [R][N^{(n)}Q])^{-1}, \tag{26}$$

$$\tilde{Q} = -[N^{(n)}Q]\tilde{S}, \tag{27}$$

$$\tilde{R} = -\tilde{S}[RN^{(n)}], \tag{28}$$

$$\tilde{P} = N^{(n)} + [N^{(n)}Q]\tilde{S}[RN^{(n)}]. \tag{29}$$

It follows from Eq. (25) that the calculation of the determinant ratio for removing a spin is $O(1)$, since it is just element $\tilde{S}$, and from the above formulas we also immediately find the definition of the reduced matrix:

$$N^{(n)} = \tilde{P} - \frac{[\tilde{Q}][\tilde{R}]}{\tilde{S}}. \tag{30}$$

D. Measurement of the Green's function

To compute the contribution of a configuration c to the Green's function measurement (6), we insert a creation operator $d^\dagger$ at time 0 and an annihilation operator d at time τ,

$$g_\sigma^c(\tau) = \frac{1}{w_c} Tr\left[e^{-(\beta-\tau_n)H_1} e^{\gamma s_n(n_\uparrow - n_\downarrow)} \dots e^{-(\tau_{k+1}-\tau)H_1} d_\sigma e^{-(\tau-\tau_k)H_1} \dots e^{\gamma s_1(n_\uparrow - n_\downarrow)} e^{-\tau_1 H_1} d_\sigma^\dagger\right] \left(\frac{Kd\tau}{2\beta}\right)^n. \tag{31}$$

with w_c given in Eq. (14). The same steps as in section II A (Wick's theorem) then lead to the expression

$$\begin{aligned}
g_\sigma^c(\tau) &= \frac{1}{\det N_\sigma^{-1} \det N_{\bar{\sigma}}^{-1}} \det N_{\bar{\sigma}}^{-1} \det \begin{pmatrix} (N_\sigma^{(n)})^{-1} & [g_{0\sigma}(\tau_i)] \\ -[g_{0\sigma}(\tau-\tau_j)(e^{\Gamma_{\sigma j}}-1)] & g_{0\sigma}(\tau) \end{pmatrix} \\
&= g_{0\sigma}(\tau) + [g_{0\sigma}(\tau-\tau_j)(e^{\Gamma_{\sigma j}}-1)]N_\sigma^{(n)}[g_{0\sigma}(\tau_i)]. \tag{32}
\end{aligned}$$

The second equality follows from Eq. (25) and square brackets denote vectors of length n.

To avoid unnecessary and time consuming summations during the Monte Carlo simulations, we only accumulate the quantity

$$S_\sigma(\tilde{\tau}) \equiv \sum_{k=1}^{n} \delta(\tilde{\tau} - \tau_k) \sum_{l=1}^{n} \left[(e^{\Gamma_\sigma} - I)N_\sigma\right]_{kl} g_{0\sigma}(\tau_l), \tag{33}$$

binning the time points $\tilde{\tau}$ on a fine grid. After the simulation is completed, the Green's function is computed as

$$g_\sigma(\tau) = g_{0\sigma}(\tau) + \int_0^\beta d\tilde{\tau} g_{0\sigma}(\tau - \tilde{\tau})\langle S_\sigma(\tilde{\tau})\rangle. \tag{34}$$

E. Expansion order and role of the parameter K

It follows from Eq. (11) that

$$
\begin{aligned}
\langle -H_2 \rangle &= \frac{1}{\beta} \int_0^\beta d\tau \langle -H(\tau) \rangle \\
&= \frac{1}{\beta} \frac{1}{Z} \sum_{n=0}^{\infty} \frac{n+1}{(n+1)!} \int_0^\beta d\tau \int_0^\beta d\tau_1 \dots \int_0^\beta d\tau_n Tr \left[e^{-\beta H_1} T(-H_2(\tau))(-H_2(\tau_n)) \dots (-H_2(\tau_1)) \right] \\
&= \frac{1}{\beta} \frac{1}{Z} \sum_c n(c) w_c = \frac{1}{\beta} \langle n \rangle,
\end{aligned}
\tag{35}
$$

and because $\langle -H_2 \rangle = K/\beta - U \langle n_\uparrow n_\downarrow - (n_\uparrow + n_\downarrow)/2 \rangle$ we therefore find that the average perturbation order $\langle n \rangle$ is related to the parameter K and the potential energy by

$$
\langle n \rangle = K - \beta U \langle n_\uparrow n_\downarrow - (n_\uparrow + n_\downarrow)/2 \rangle.
\tag{36}
$$

Increasing K leads to a higher perturbation order (and thus slower matrix updates), but through Eq. (13) also to a smaller value of γ and thus to less polarization of the auxiliary spins. A K of the order 1 appears to work well [2]. We also learn from Eq. 36 that the average perturbation order grows essentially proportional to U (as expected for a weak-coupling method), and proportional to inverse temperature.

III. "STRONG COUPLING" APPROACH - EXPANSION IN HYBRIDIZATION

The second diagrammatic method, which is in many ways complementary to the weak-coupling approach, is based on an expansion of the partition function in powers of the impurity-bath hybridization V. It has been presented for the Anderson impurity model in Ref. [6] and and generalized to arbitrary

A. Monte Carlo configurations

Here, we decompose the Hamiltonian as $H_2 = H_{\text{mix}}$ and $H_1 = H - H_2 = H_0 + H_U + H_{\text{bath}}$. Since $H_2 \equiv H_2^{d^\dagger} + H_2^d = \sum_{\sigma,p} V_p^\sigma d_\sigma^\dagger a_{p,\sigma} + \sum_{\sigma,p'} V_{p'}^{\sigma*} d_\sigma a_{p,\sigma}^\dagger$ has two terms, corresponding to electrons hopping from the bath to the impurity and from the impurity back to the bath, only even perturbation orders contribute to Eq. (10). Furthermore, at perturbation order $2n$ only the $(2n)!/(n!)^2$ terms corresponding to n creation operators $d^\dagger$ and n annihilation

operators d will contribute. We can therefore write the partition function as a sum over configurations $c = \{\tau_1, \ldots, \tau_n; \tau_1', \ldots, \tau_n'\}$:

$$Z = \sum_{n=0}^{\infty} \int_0^{\beta} d\tau_1 \ldots \int_{\tau_{n-1}}^{\beta} d\tau_n \int_0^{\beta} d\tau_1' \ldots \int_{\tau_{n-1}'}^{\beta} d\tau_n' Tr\left[e^{-\beta H_1} T H_2^d(\tau_n) H_2^{d\dagger}(\tau_n') \ldots H_2^d(\tau_1) H_2^{d\dagger}(\tau_1')\right].$$

$$(37)$$

Since the time evolution of the Anderson model (given by H_1) does not rotate the spin, there is an additional constraint, namely that both for spin up and spin down, there is an equal number of creation and annihilation operators. Taking this into account and writing out the expressions for H_2^d and $H_2^{d\dagger}$ explicitly, we find

$$Z = \sum_{\{n_\sigma\}} \prod_\sigma \int_0^{\beta} d\tau_1^{\sigma} \ldots \int_{\tau_{n_\sigma-1}^{\sigma}}^{\beta} d\tau_{n_\sigma}^{\sigma} \int_0^{\beta} d\tau_1'^{\sigma} \ldots \int_{\tau_{n_\sigma-1}'^{\sigma}}^{\beta} d\tau_{n_\sigma}'^{\sigma}$$

$$\times Tr\left[e^{-\beta H_1} T \prod_\sigma \sum_{p_1,\ldots,p_{n_\sigma}} \sum_{p_1',\ldots,p_{n_\sigma}'} V_{p_1}^{\sigma} V_{p_1'}^{\sigma*} \ldots V_{p_{n_\sigma}}^{\sigma} V_{p_{n_\sigma}'}^{\sigma*}\right.$$

$$\left. d_\sigma(\tau_{n_\sigma}^{\sigma}) a_{\sigma,p_{n_\sigma}}^{\dagger}(\tau_{n_\sigma}^{\sigma}) a_{\sigma,p_{n_\sigma}'}(\tau_{n_\sigma}'^{\sigma}) d_\sigma^{\dagger}(\tau_{n_\sigma}'^{\sigma}) \ldots d_\sigma(\tau_1^{\sigma}) a_{\sigma,p_1}^{\dagger}(\tau_1^{\sigma}) a_{\sigma,p_1'}(\tau_1'^{\sigma}) d_\sigma^{\dagger}(\tau_1'^{\sigma})\right]. \quad (38)$$

Now, because the d and a operate on different spaces and H_1 does not mix the impurity and bath states, we can separate the bath and the impurity and write

$$Z = Z_{\text{bath}} \sum_{\{n_\sigma\}} \prod_\sigma \int_0^{\beta} d\tau_1^{\sigma} \ldots \int_{\tau_{n_\sigma-1}^{\sigma}}^{\beta} d\tau_{n_\sigma}^{\sigma} \int_0^{\beta} d\tau_1'^{\sigma} \ldots \int_{\tau_{n_\sigma-1}'^{\sigma}}^{\beta} d\tau_{n_\sigma}'^{\sigma}$$

$$\times Tr_d\left[e^{-\beta H_{\text{loc}}} T \prod_\sigma d_\sigma(\tau_{n_\sigma}^{\sigma}) d_\sigma^{\dagger}(\tau_{n_\sigma}'^{\sigma}) \ldots d_\sigma(\tau_1^{\sigma}) d_\sigma^{\dagger}(\tau_1'^{\sigma})\right]$$

$$\times \frac{1}{Z_{\text{bath}}} Tr_a\left[e^{-\beta H_{\text{bath}}} T \prod_\sigma \sum_{p_1,\ldots,p_{n_\sigma}} \sum_{p_1',\ldots,p_{n_\sigma}'} V_{p_1}^{\sigma} V_{p_1'}^{\sigma*} \ldots V_{p_{n_\sigma}}^{\sigma} V_{p_{n_\sigma}'}^{\sigma*}\right.$$

$$\left. a_{\sigma,p_{n_\sigma}}^{\dagger}(\tau_{n_\sigma}^{\sigma}) a_{\sigma,p_{n_\sigma}'}(\tau_{n_\sigma}'^{\sigma}) \ldots a_{\sigma,p_1}^{\dagger}(\tau_1^{\sigma}) a_{\sigma,p_1'}(\tau_1'^{\sigma})\right], \quad (39)$$

where $Z_{\text{bath}} = Tr_a e^{-\beta H_{\text{bath}}}$, and $H_{\text{loc}} = H_0 + H_U$. Because the bath is non-interacting, there is a Wick theorem for the bath and $Tr_a[\ldots]$ can again be expressed as the determinant of some matrix, whose size is equal to the perturbation order. To find the elements of this matrix, it is useful to consider the lowest perturbation order, $n_\sigma = 1$, $n_{\bar{\sigma}} = 0$. In this case

$$\sum_{p_1} \sum_{p_1'} V_{p_1}^{\sigma} V_{p_1'}^{\sigma*} \frac{1}{Z_{\text{bath}}} Tr_a\left[e^{-\beta H_{\text{bath}}} T a_{\sigma,p_1}^{\dagger}(\tau_1^{\sigma}) a_{\sigma,p_1'}(\tau_1'^{\sigma})\right]$$

$$= \sum_{p_1} \frac{|V_{p_1}^{\sigma}|^2}{e^{-\epsilon_{p_1}\beta}+1} \begin{cases} e^{-\epsilon_{p_1}(\beta-(\tau_1^{\sigma}-\tau_1'^{\sigma}))} & \tau_1^{\sigma} > \tau_1'^{\sigma} \\ -e^{-\epsilon_{p_1}(\tau_1'^{\sigma}-\tau_1^{\sigma})} & \tau_1^{\sigma} < \tau_1'^{\sigma} \end{cases}. \quad (40)$$

Note that $Z_{\text{bath}} = \prod_\sigma \prod_p (e^{-\epsilon_p \beta} + 1)$. Introducing the β-antiperiodic *hybridization function*

$$F_\sigma(\tau) = \sum_p \frac{|V_p|^2}{e^{-\epsilon_p \beta} + 1} \begin{cases} e^{-\epsilon_p(\beta-\tau)} & \tau > 0 \\ -e^{-\epsilon_p(-\tau)} & \tau < 0 \end{cases}, \qquad F_\sigma(-i\omega_n) = \sum_p \frac{|V_p^\sigma|^2}{i\omega_n - \epsilon_p}, \qquad (41)$$

which is related to the non-interacting Green's function $G_{0\sigma}$ of section II by $F_\sigma(-i\omega_n) = i\omega_n + \mu - U/2 - G_{0\sigma}(i\omega_n)^{-1}$, the first order result becomes $F_\sigma(\tau_1^\sigma - \tau_1'^\sigma)$. For higher orders, one obtains

$$\frac{1}{Z_{\text{bath}}} Tr_a \Big[e^{-\beta H_{\text{bath}}} T \prod_\sigma \sum_{p_1,\ldots,p_{n_\sigma}} \sum_{p_1',\ldots,p_{n_\sigma}'} V_{p_1}^\sigma V_{p_1'}^{\sigma*} \ldots V_{p_{n_\sigma}}^\sigma V_{p_{n_\sigma}'}^{\sigma*}$$

$$a_{\sigma,p_{n_\sigma}}^\dagger(\tau_{n_\sigma}^\sigma) a_{\sigma,p_{n_\sigma}'}(\tau_{n_\sigma}'^\sigma) \ldots a_{\sigma,p_1}^\dagger(\tau_1^\sigma) a_{\sigma,p_1'}(\tau_1'^\sigma) \Big] = \prod_\sigma \det M_\sigma^{-1}, \qquad (42)$$

where M_σ^{-1} is a $(n_\sigma \times n_\sigma)$ matrix with elements

$$M_\sigma^{-1}(i,j) = F_\sigma(\tau_i^\sigma - \tau_j'^\sigma). \qquad (43)$$

In the hybridization expansion method, the configuration space consists of all sequences $c = \{\tau_1^\uparrow, \ldots, \tau_{n_\uparrow}^\uparrow; \tau_1'^\uparrow, \ldots, \tau_{n_\uparrow}'^\uparrow | \tau_1^\downarrow, \ldots, \tau_{n_\downarrow}^\downarrow; \tau_1'^\downarrow, \ldots, \tau_{n_\downarrow}'^\downarrow \}$, of $n_\uparrow$ creation and annihilation operators for spin up ($n_\uparrow = 0, 1, \ldots$), and $n_\downarrow$ creation and annihilation operators for spin down ($n_\downarrow = 0, 1, \ldots$). The weight of this configuration is

$$w_c = Z_{\text{bath}} Tr_d \Big[e^{-\beta H_{\text{loc}}} T \prod_\sigma d_\sigma(\tau_{n_\sigma}^\sigma) d_\sigma^\dagger(\tau_{n_\sigma}'^\sigma) \ldots d_\sigma(\tau_1^\sigma) d_\sigma^\dagger(\tau_1'^\sigma) \Big]$$

$$\times \prod_\sigma \det M_\sigma^{-1}(\tau_1^\sigma, \ldots, \tau_{n_\sigma}^\sigma; \tau_1'^\sigma, \ldots, \tau_{n_\sigma}'^\sigma)(d\tau)^{2n_\sigma}. \qquad (44)$$

The trace factor represents the contribution of the impurity, which fluctuates between different quantum states, as electrons hop in and out. The determinants resum all the bath evolutions which are compatible with the given sequence of transitions.

To evaluate the trace factor, we use the eigenbasis of H_{loc}, which is $|0\rangle$ (energy $E_0 = 0$), $|\uparrow\rangle, |\downarrow\rangle$ (energy $E_1 = -\mu$) and $|\uparrow\downarrow\rangle$ (energy $E_2 = U - 2\mu$). In this basis, the time evolution operator $e^{-\tau H_{\text{loc}}} = \text{diag}(e^{-\tau E_0}, e^{-\tau E_1}, e^{-\tau E_1}, e^{-\tau E_2})$ is diagonal while the operators d_σ and $d_\sigma^\dagger$ will produce transitions between eigenstates with amplitude ± 1.

Because the time evolution does not flip the spin, the creation and annihilation operators for given spin have to alternate. This allows us to separate the operators for spin up from those for spin down and to depict the time evolution by a collection of segments (each

segment representing a time interval in which an electron of spin up or down resides on the impurity). At each time, the eigenstate of the impurity follows immediately from the segment representation and we can easily compute the trace factor as

$$Tr_d\left[e^{-\beta H_{\rm loc}}T\prod_\sigma d_\sigma(\tau^\sigma_{n_\sigma})d^\dagger_\sigma(\tau'^\sigma_{n_\sigma})\dots d_\sigma(\tau^\sigma_1)d^\dagger_\sigma(\tau'^\sigma_1)\right] = \exp\left[\mu(l_\uparrow + l_\downarrow) - Ul_{\rm overlap}\right], \qquad (45)$$

with l_σ the total "length" of the segments for spin σ and $l_{\rm overlap}$ the total length of the overlap between up and down segments.

B.   Sampling procedure and detailed balance

For ergodicity, it is sufficient to insert and remove pairs of creation and annihilation operators (segments or anti-segments) for spin up and down. One possible strategy for inserting a segment is the following: we pick a random time in $[0, \beta)$ for the creation operator. If it falls on an existing segment, the impurity is already occupied and the move is rejected. If it falls on an empty space, we compute $l_{\rm max}$, the length from this position to the next (in the direction of increasing τ) segment. If there are no segments, $l_{\rm max} = \beta$. The position of the new annihilation operator is then chosen randomly in this interval of length $l_{\rm max}$ (see Fig. 3). If we propose to remove a randomly chosen segment for this spin, then the proposal probabilities are

$$p^{\rm prop}(n_\sigma \to n_\sigma + 1) = \frac{d\tau}{\beta}\frac{d\tau}{l_{\rm max}}, \qquad (46)$$

$$p^{\rm prop}(n_\sigma + 1 \to n_\sigma) = \frac{1}{n_\sigma + 1}, \qquad (47)$$

and the ratio of acceptance probabilities therefore becomes

$$\frac{p^{\rm acc}(n_\sigma \to n_\sigma + 1)}{p^{\rm acc}(n_\sigma + 1 \to n_\sigma)} = \frac{\beta l_{\rm max}}{n_\sigma + 1}e^{\mu l_{\rm new} - U\delta l_{\rm overlap}}\frac{|\det(M_\sigma^{(n_\sigma+1)})^{-1}|}{|\det(M_\sigma^{(n_\sigma)})^{-1}|}. \qquad (48)$$

Here, $l_{\rm new}$ is the length of the new segment, and $\delta l_{\rm overlap}$ the change in the overlap. Again, we compute the ratio of determinants using the fast update formulas discussed in section II.

C.   Measurement of the Green's function

The strategy proposed in Ref. [6] is to create configurations which contribute to the Green's function measurement by decoupling the bath from a given pair of creation and
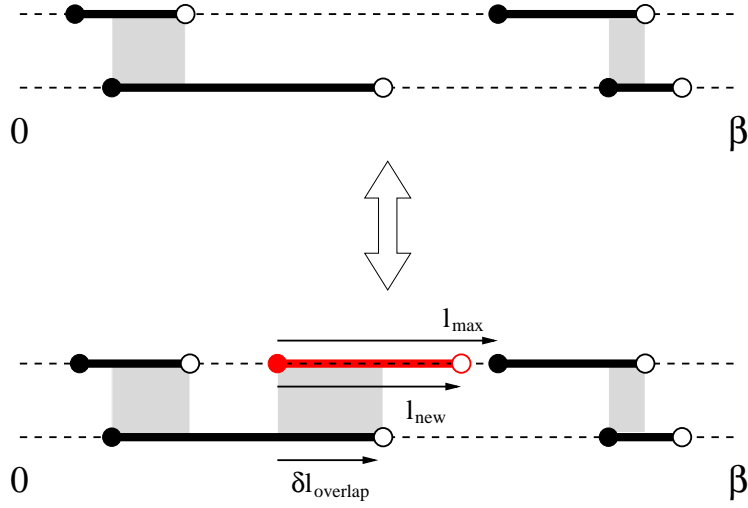
FIG. 3: Local update in the "segment" picture. The two segment configurations correspond to spin up and spin down. Each segment depicts a time interval in which an electron of the corresponding spin resides on the impurity (the end points are the locations of the operators $d^\dagger$ and d). We increase the perturbation order by adding a segment or anti-segment of random length for random spin. The perturbation order is decreased by removing a randomly chosen segment.

annihilation operators in c. The idea is to write

$$g(\tau) = \frac{1}{Z}\sum_c w_c^{d(\tau)d^\dagger(0)} = \frac{1}{Z}\sum_c w_c^{(\tau,0)}\frac{w_c^{d(\tau)d^\dagger(0)}}{w_c^{(\tau,0)}}, \tag{49}$$

where $w_c^{d(\tau)d^\dagger(0)}$ denotes the weight of configuration c with and additional operator $d^\dagger(0)$ and $d(\tau)$ in the trace factor, and $w_c^{(\tau,0)}$ the complete weight corresponding to the enlarged operator sequence (including enlarged hybridization determinants). Since the trace factors of both weights are identical, and $\det M_c^{-1}$ is a minor of $\det(M_c^{(\tau,0)})^{-1}$, we find

$$\frac{w_c^{d(\tau)d^\dagger(0)}}{w_c^{(\tau,0)}} = \frac{\det M_c^{-1}}{\det(M_c^{(\tau,0)})^{-1}} = (M_c^{(\tau,0)})_{j,i}, \tag{50}$$

with i and j denoting the row and column corresponding to the new operators $d^\dagger$ and d in the enlarged $(M_c^{(\tau,0)})^{-1}$. To transform the sum over c into a sum over configurations $\tilde{c} = \{c, \tau_i, \tau_j'\}$, the new operators must be free to be anywhere on the imaginary time interval, which (due to translational invariance) yields a factor $\frac{1}{\beta}\Delta(\tau, \tau_i - \tau_j')$, with

$$\Delta(\tau, \tau') = \begin{cases} \delta(\tau - \tau') & \tau' > 0 \\ -\delta(\tau - \tau' - \beta) & \tau' < 0 \end{cases}. \tag{51}$$

Hence, the measurement of the Green's function becomes

$$g(\tau) = \frac{1}{Z} \sum_{\tilde{c}} w_{\tilde{c}} \sum_{i,j} \frac{1}{\beta} \Delta(\tau, \tau_i - \tau'_j)(M_{\tilde{c}})_{j,i} = \left\langle \sum_{i,j} \frac{1}{\beta} \Delta(\tau, \tau_i - \tau'_j) M_{j,i} \right\rangle. \qquad (52)$$

Note that if we let all the integrals run from 0 to β, there is a factor $1/(n!)^2$ in w_c and $1/((n+1)!)^2$ in $w_{\tilde{c}}$, with n the size of M_c. Changing from a sum over c to a sum over $\tilde{c}$ therefore adds a factor $(n+1)^2$ if we restrict the measurement to a specific pair of $d^\dagger$ and d. Equivalently, we can sum over all the $(n+1)^2$ pairs of operators in the enlarged configuration.

D. Generalization - Matrix formalism

It is obvious from the derivation in section III A that the hybridization expansion formalism is applicable to general classes of impurity models. Because the trace factor in the weight (44) is computed exactly, H_{loc} can contain essentially arbitrary interactions and degrees of freedom (including spins, which cannot be treated using the weak-coupling method). For example, the method has been used in Ref. [7] for a dynamical mean field investigation of the Kondo lattice model, and in Ref. [8] for a study of the $t - J$ model.

For multi-orbital impurity models with density-density interaction, the segment formalism is still applicable: we have now a collection of segments for each *flavor* α (orbital, spin) and the trace factor can still be computed from the length of the segments (chemical potential contribution) and the overlaps between segments of different flavor (interaction terms).

If H_{loc} is not diagonal in the occupation number basis defined by the $d^\dagger_\alpha$, the calculation of $Tr_d\left[e^{-\beta H_{\mathrm{loc}}} T \prod_\alpha d_\alpha(\tau^\alpha_{n_\alpha}) d^\dagger_\alpha(\tau'^\alpha_{n_\alpha}) \dots d_\sigma(\tau^\alpha_1) d^\dagger_\alpha(\tau'^\alpha_1)\right]$ becomes more involved. We now have to compute the trace explicitly in some basis of H_{loc} – preferably the eigenbasis, because then the time evolution operators $e^{-H_{\mathrm{loc}}\tau}$ become diagonal. The operators d_α and $d^\dagger_\alpha$ are expressed as matrices in this eigenbasis, and the evaluation of the trace factor thus involves the multiplication of matrices whose size is equal the size of the Hilbert space of H_{loc}. Since the dimension of the Hilbert space grows exponentially with the number of flavors, the calculation of the trace factor becomes the computational bottleneck of the simulation, and the matrix formalism is therefore restricted to a relatively small number of flavors ($\lesssim 10$).

An important point, explained in the paper by Haule [8], is the use of *conserved quantum numbers* (typically particle number for spin up and spin down, momentum, ...). If the eigen-

states of H_{loc} are grouped according to these quantum numbers, the operator matrices will acquire a sparse block structure, because for example $d^{\dagger}_{\uparrow,q}$ will connect the states corresponding to quantum numbers $m = \{n_{\uparrow}, n_{\downarrow}, K\}$ to those corresponding to $m' = \{n_{\uparrow}+1, n_{\downarrow}, K+q\}$ (if they exist). Checking the compatibility of the operator sequence with a given starting block furthermore allows one to find the (potentially) contributing quantum number sectors without any matrix multiplications. The evaluation of the trace is thus reduced to a block matrix multiplication of the form

$$\sum_{\text{contr.}m} Tr_m \Big[\ldots (O)_{m'',m'} (e^{-(\tau'-\tau)H_{\text{loc}}})_{m'} (O)_{m',m} (e^{-\tau H_{\text{loc}}})_m \Big]. \tag{53}$$

IV. COMPARISON BETWEEN THE TWO APPROACHES

The weak and "strong" coupling methods are in many ways complementary and their respective strengths/weaknesses results from the scaling of the computational effort with interaction strength and system size. For the Anderson impurity model considered in these notes, the U dependence of the average perturbation order is shown in Fig. 4 (these are dynamical mean field theory calculations for a one-band Hubbard model, taken from Ref. [9]). In the weak-coupling algorithms, where the average perturbation order is related to the potential energy, one finds a roughly linear increase of the perturbation order with U. In the hybridization-expansion method, the average perturbation order is related to the kinetic energy, and decreases as the interaction strength increases. Thus, in single site models with only density density interactions (where the evaluation of the trace factor in Eq. (44) is cheap), the hybridization expansion method beats the weak coupling method in the strong coupling regime.

For more complicated models, which require the matrix formalism discussed in section III D, the hybridization expansion method scales exponentially with system size, and can only be applied to relatively small systems.[10] Here, the weak-coupling approach – if applicable – becomes the method of choice. Table I gives a summary of the different scalings (assuming diagonal hybridization) and indicates which solver is appropriate for which type of problem.
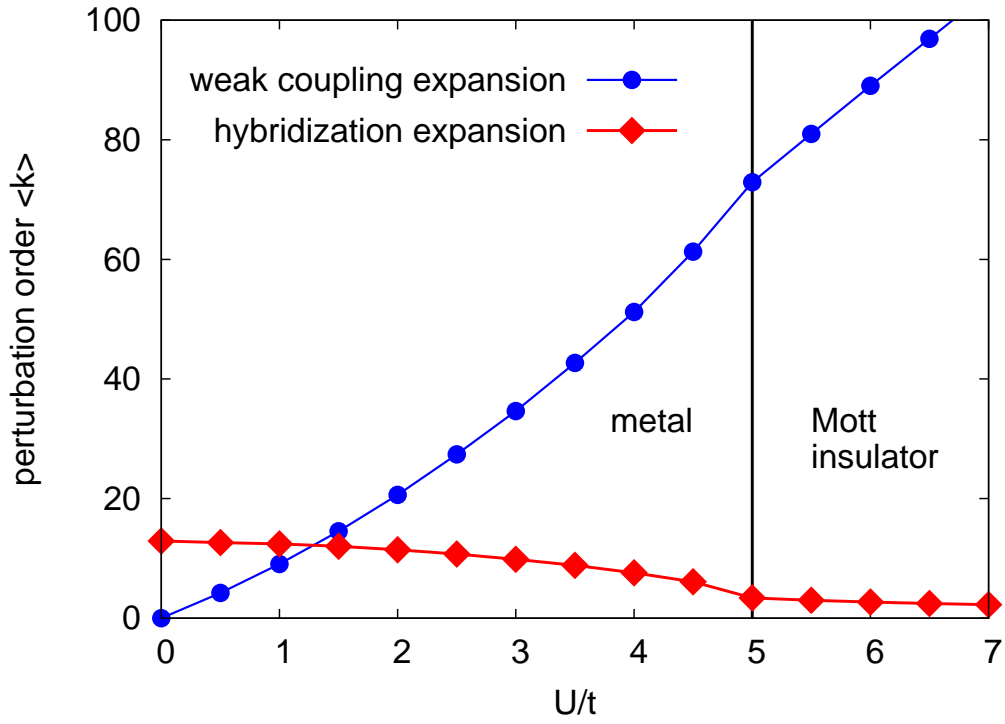
FIG. 4: Average perturbation order for the weak-coupling and strong coupling (hybridization expansion) algorithm. These results correspond to the DMFT solution of the one-band Hubbard model with semi-circular density of states of bandwidth $4t$, and temperature $\beta = 1/T = 30$. The bath is therefore different for each data point.

solver	scaling with β	scaling with L	use for
weak-coupling	β^3	L^3	impurity clusters with density-density interactions and hopping
hybridization expansion (segment formulation)	β^3	L	single site multi-orbital models with density-density interaction
hybridization expansion (matrix formulation)	β	$\exp(L)$	single site multi-orbital models with general U_{ijkl}

TABLE I: Scaling of the different impurity solvers with inverse temperature and system size.

Acknowledgments

---

[1] A. N. Rubtsov, V. V. Savkin and A. I. Lichtenstein, Phys. Rev. B **72**, 035122 (2005).

[2] E. Gull, P. Werner, O. Parcollet and M. Troyer, Europhys. Lett. **82** 57003 (2008).

[3] S. M. A. Rombouts, K. Heyde, and N. Jachowicz, Phys. Rev. Lett. **82**, 4155 (1999).

[4] J. E. Hirsch and R. M. Fye, Phys. Rev. Lett. **56**, 2521 (1986).

[5] W. T. Vetterling, B. P. Flannery, W. H. Press, and S. A. Teukolski, Numerical Recipes in FORTRAN - TheArt of Scientific Computing - Second Edition (University Press, Cambridge, 1992), ISBN0-521-43064-X.

[6] P. Werner, A. Comanac, L. de' Medici, M. Troyer and A. J. Millis, Phys. Rev. Lett. **97**, 076405 (2006).

[7] P. Werner and A. J. Millis, Phys. Rev. B **74**, 155107 (2006).

[8] K. Haule, Phys. Rev. B **75**, 155113 (2007).

[9] E. Gull, P. Werner, A. J. Millis, and M. Troyer, Phys. Rev. B **76**, 235123 (2007).

[10] While the calculation of the trace over atomic states is time consuming, it also yields useful information about the system (histogram of visited states).